

MD/GE - Molecular dynamics simulation and lattice energy of argon

Protocol for the PC 2 lab course by
Vincent Kümmerle & Elvis Gnaglo & Julian Brügger

University of Stuttgart

authors: Vincent Kümmerle, 3712667
st187541@stud.uni-stuttgart.de

Elvis Gnaglo, 3710504
st189318@stud.uni-stuttgart.de

Julian Brügger,
st190010@stud.uni-stuttgart.de

group number: A05

date of experiment: 10.12.2025

supervisor: Xiangyin Tan

submission date: December 14, 2025

Abstract:

Contents

1 Theory	1
2 Procedure	3
2.1 Molecular Dynamics Simulations	3
2.2 Lattice Energy of Argon	3
3 Results	5
4 Analysis	6
4.1 Molecular Dynamics Simulations	6
4.1.1 Isochor simulations	6
4.1.2 Isobaric simulations	8
4.2 Lattice Energy of Argon	8
5 Error Discussion	8
6 Conclusion	8
7 References	8

1 Theory

Molecular dynamics simulations (MDS) are used to visualize spatial movements of atoms and molecules. For that a numerical algorithm can determine the positions r_i and momentums p_i for each particle i .^[1] A proven algorithm is the Velocity-Verlet algorithm, which assigns each particle a random starting position and velocity at first before calculating the new positions and velocities a small time step later. That is achieved by calculating the new accelerations using the provided potential, e.g. lennard-Jones potential. So for the computation of particle trajectories in MDS the equation of motion is integrated and then the forces induced by potentials are calculated. To approximate the intermolecular interactions between particles, the Lennard-Jones potential (LJ-potential) V_{ij} with equation 1 is used.^[1]

$$V(r_{ij}) = 4\epsilon_0 \left[\left(\frac{\sigma_0}{r_{ij}} \right)^{12} - \left(\frac{\sigma_0}{r_{ij}} \right)^6 \right], \quad (1)$$

σ_0 describes the minimum distance, r_{ij} the distance between particle i and j and ϵ_0 the depth of the potential well at the equilibrium distance r_e , which can be seen in figure 1. The positive part with a twelfth power-term characterizes the repulsive interactions to the nearest neighbours, whereas the negative part with a sixth power-term characterizes the attractive electrostatic interactions.^[1]

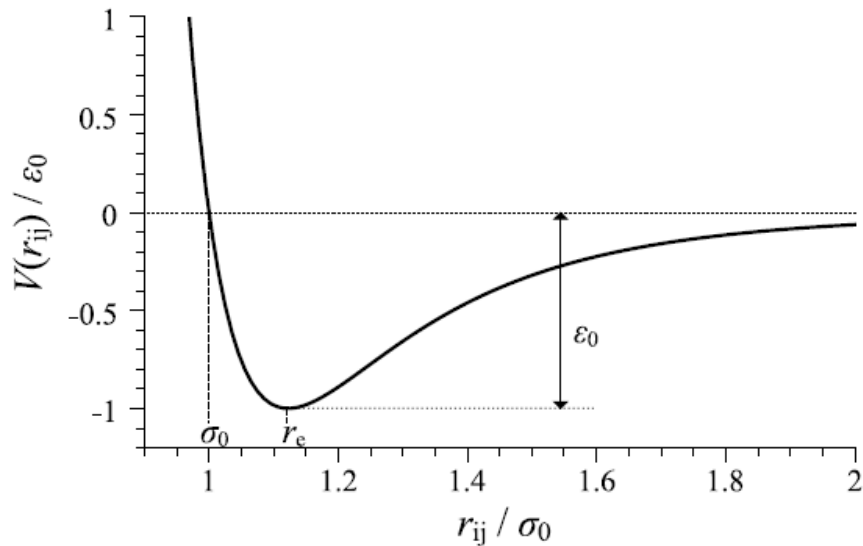


Figure 1: Potential curve of a Lennard-Jones potential V_{ij} depending on the particle distance r_{ij} .^[1]

In MDS reduced properties are used to describe thermodynamical states by defining units and setting the value to 1.0 for shorter calculation times. When using the LJ-potential the fundamental units ϵ_0 , σ_0 and the mass m are set to 1.0. In the experiment the reduced units of pressure p^* and temperature T^* are used, which can be calculated with equation 2 and 3.

$$T^* = \frac{k_B T}{\varepsilon_0} \quad (2)$$

$$p^* = \frac{p \sigma_0^3}{\varepsilon_0} \quad (3)$$

In an isolated system, where the gaseous and solid phase are in equilibrium and the volume of the gas is much bigger than the volume of the liquid, the Clausius-Clapeyron equation 4 can be used to describe the dependence of the sublimation pressure p on the temperature T .

$$\ln p = -\frac{\Delta H_{\text{sub}}}{RT} + C \quad (4)$$

The enthalpy of sublimation ΔH_{sub} can be determined by plotting $\ln p$ against $1/T$. Argon behaves like an ideal gas at 70 K and the internal energy ΔU during a phase transition from solid to gaseous is the difference of the corresponding internal energies. Because the translational energy of gaseous argon corresponds to the kinetic theory of gases, the total internal energy of the solid U_s can be calculated with equation 6.

$$U_s = \frac{5}{2}RT - \Delta H \quad (5)$$

U_s consists of two parts, which are described in equation 5.^[1]

$$\Delta U_s = U_{\text{lattice}} + U_{\text{vib}} \quad (6)$$

The first part corresponds with the potential energy of argon atoms at rest on their lattice planes, whereas the second part is the vibrational energy of the atoms. For the calculation of U_{vib} , Debyes theory is used, which states that the crystal is composed as independent vibrating lattice atoms with varying frequencies. For that the equation 7 shows the connection between the vibrational energy and the Debye-temperature Θ_D .

$$U_{\text{vib}} = \frac{9}{8}R\Theta_D + 3RTD \left(\frac{\Theta_D}{T} \right) \quad (7)$$

To calculate the theoretical value of the lattice energy, equation 8 can be used, which is derived from the pair potentials $V_{ij}(r_{ij})$ in the LJ-potential equation 1.

$$U_{\text{lattice}}(s) = 2N_A\varepsilon_0 \left[12.132 \left(\frac{\sigma_0}{a} \right)^{12} - 14.454 \left(\frac{\sigma_0}{a} \right)^6 \right] \quad (8)$$

N_A is Avogadro's constant and a the distance between atoms. For Argon the best values, which were determined from other properties of the gas, are $\varepsilon_0 = 1.643 \times 10^{-21}$ J and $\sigma_0 = 3.41 \times 10^{-10}$ m.^[2]

2 Procedure

2.1 Molecular Dynamics Simulations

The computational work consisted of three sequential simulation tasks carried out using pre-written Python programs. In the first task, the behavior of argon particles was investigated under conditions of increasing temperature at constant pressure. The simulation focused on visualizing particle motion and the associated expansion of the system volume. To achieve this, the number of cooling steps was gradually increased, followed by an adjustment of the interaction potential depth in order to observe its influence on the system dynamics.

In the second task, the sublimation behavior of argon was studied by analyzing the relationship between temperature and pressure at constant volume. Two simulations were performed with different numerical resolutions. Initially, the system was simulated using 100 cycles with 1000 steps. In a subsequent run, the parameters were increased to 200 cycles and 4000 steps. The resulting pressure–temperature dependence obtained from the simulations was then compared with the experimental measurements.

The third task addressed the temperature dependence of the system volume. For this purpose, three simulations with progressively increased numerical accuracy were carried out. The first simulation employed 50 cooling cycles with 100 cooling steps, followed by 10 cycles and 100 steps. In the second simulation, the cooling cycles were increased to 100, the cooling steps to 1000, and the number of cycles to 100. In the final simulation, the number of steps was further increased to 1000. The results of these simulations were compared in order to analyze phase transitions and to determine the melting and boiling points of argon.

2.2 Lattice Energy of Argon

The experimental setup was preassembled prior to the start of the measurements as shown in figure 2 . The experiment began with the removal of residual gases from the system. This was achieved by flushing the apparatus with nitrogen gas followed by evacuation. Subsequently, the pressure was monitored for two minutes to verify the absence of leaks. After confirming system integrity, the argon chamber was adjusted to a pressure of approximately 2500 mbar and cooled to 63.9 K, leading to a pressure decrease to about 200 mbar. At this stage, the measured pressure served as an indicator of gas purity, as significantly higher pressures would indicate contamination by other gases. Once a pressure of approximately 154 mbar was reached, the nitrogen chamber was filled to the required level and likewise cooled to 63.9 K. After all pressures stabilized, the valves were closed, the Dewar vessel was sealed, and the vacuum pump was activated. Pumping nitrogen gas from the Dewar further reduced the system temperature. Under these conditions, the pressure in the argon chamber was approximately 0.154 bar, while the nitrogen chamber reached about 0.0144 bar.

After maintaining constant pressure for an additional five minutes, the pump was switched off and the system was allowed to warm up. During the warming phase, the pressures in both chambers were recorded at intervals of 30 seconds. These data were later compared with the results from the second simulation task and used for the determination of the lattice energy of argon.

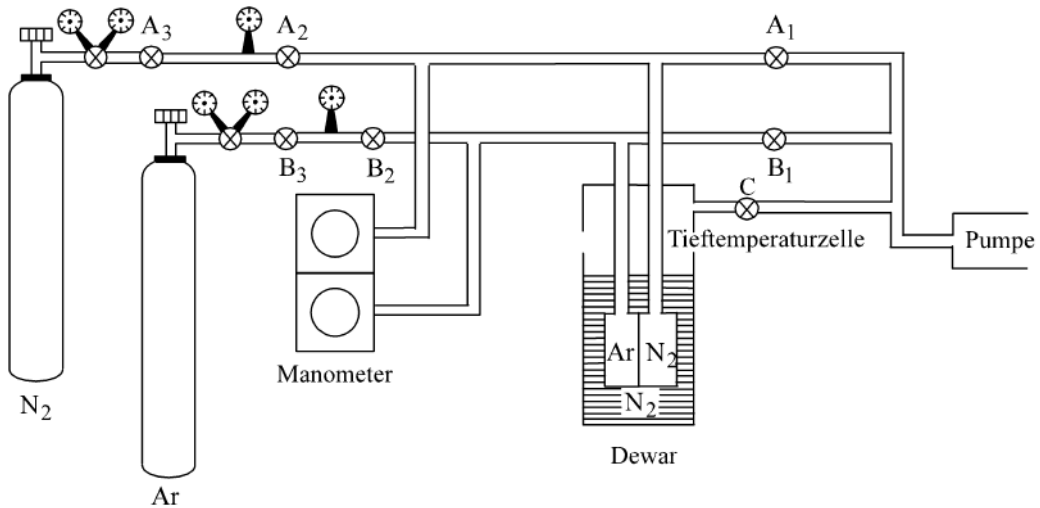


Figure 2: Scheme of the measuring apparatus.^[1]

3 Results

$$\log(p/\text{Torr}) = 7.781845 - \frac{341.619 \text{ K}}{T} - 0.0062649 \frac{T}{\text{K}} \quad (9)$$

4 Analysis

4.1 Molecular Dynamics Simulations

4.1.1 Isochor simulations

The temperatures and pressures calculated in the simulations of the second task are reported in reduced units and shown in Figure 3.

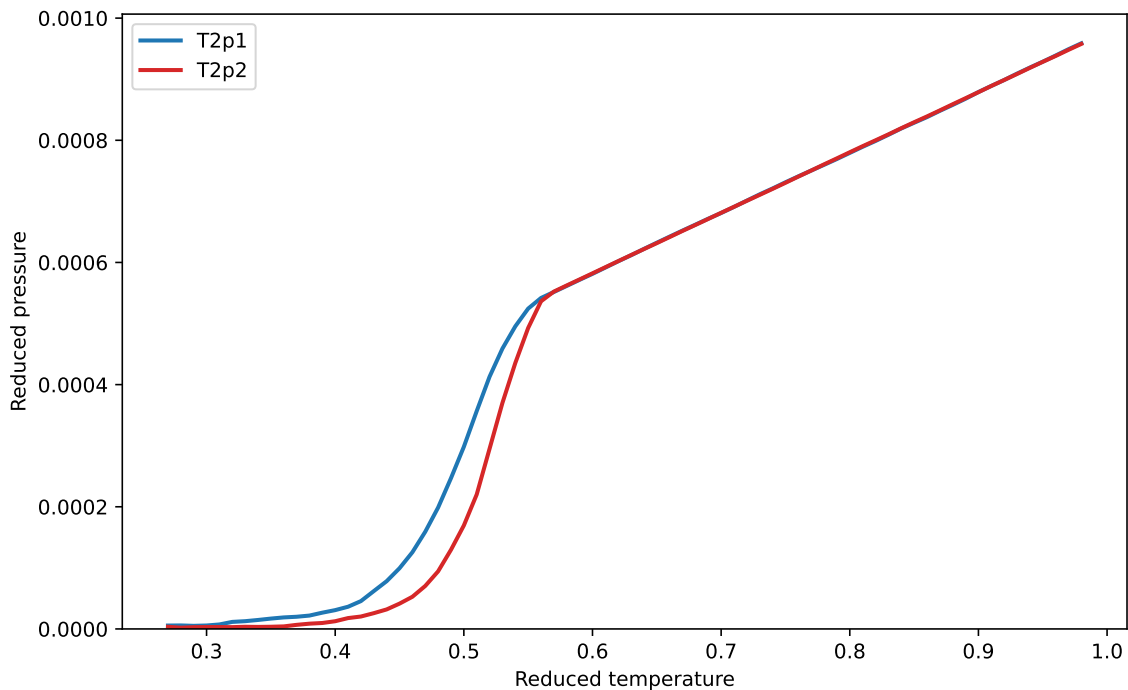


Figure 3: The reduced temperature is plotted against the reduced pressure for 100 cycles and 1000 steps (T2p1, blue) and for 200 cycles and 4000 steps (T2p2, red).

Both simulations show a very low incline before the sublimation, a steep slope while the sublimation and a transition into a linear increase of the pressure after the sublimation has ended. By increasing the number of iteration steps and the number of iterations per temperature from the first simulation T2p1 to the second T2p2, the begin of the big increase in pressure shifts to a higher temperature, while both curves lead to the same value of pressure, from which on they show the same linear increase. To compare the simulation results to the experimental results, the values of the reduced temperature and pressure are converted from reduced units into Kelvin and Pascal by using equations 2 and 3. The new values are then plotted with the experimental data from ??, which is shown Figure 4.

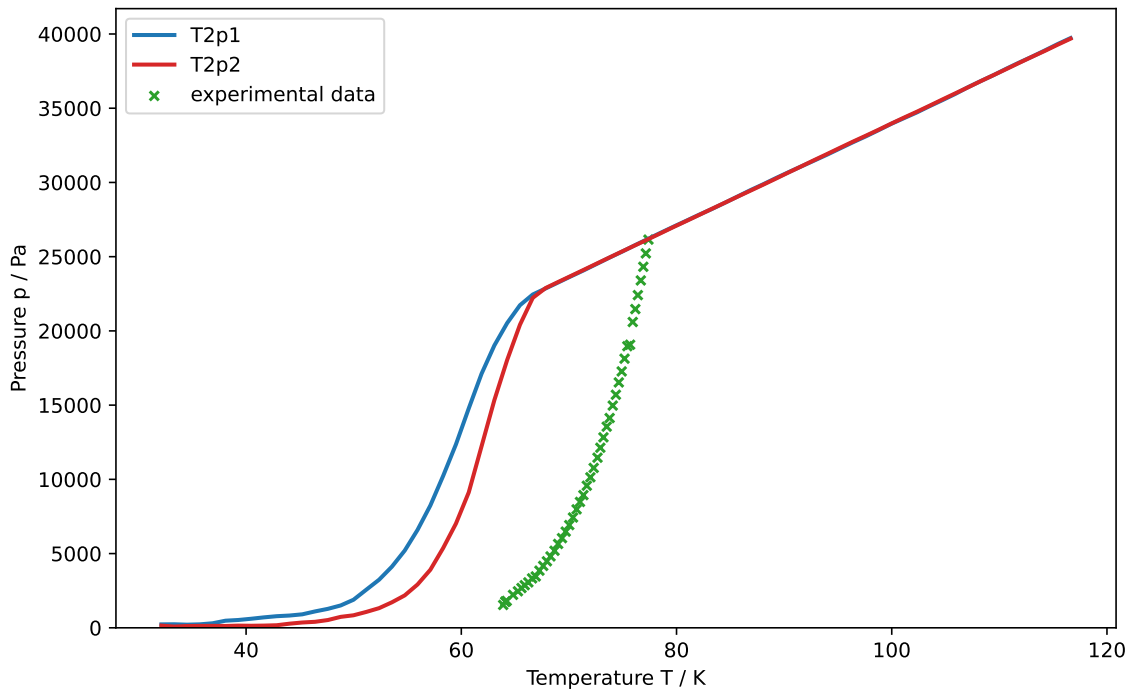


Figure 4: The converted temperature is plotted against the converted pressure from the short simulation (T2p1, blue), long simulation (T2p2, red) and the experimental values (green).

Figure 4 shows that the sublimation curve of the longer simulation with more iteration steps and cycles is closer to the experimental data than the shorter simulation. But still, the experimental sublimation curve is located around 10K higher, which can be caused by the approximation of the interactions, which are made in the Lennard-Jones potential. Furthermore, it can be concluded that a higher computation time with more iteration steps and cycles in the Velocity-Verlet algorithm would be necessary to fit the simulation values to the experimental values.

4.1.2 Isobaric simulations

4.2 Lattice Energy of Argon

5 Error Discussion

6 Conclusion

7 References

- [1] H. Dilger, *2025-pc2-script-en*, 2025.
- [2] J. O. Hirschfelder, C. F. Curtiss, R. B. Bird, *The molecular theory of gases and liquids*, John Wiley & Sons, 1964.